J Appl Phycol (2008) 20:103–111
DOI 10.1007/s10811-007-9187-2

Application of the Fourier Method to Differentiate Biological Rhythms from Stochastic Processes in the Growth of *Selenastrum capricornutum* Printz: Implications for Model Development

Barbara C. Benson · Maria T. Gutierrez-Wing · Kelly A. Rusch

Received: 10 May 2005 / Revised and accepted: 8 May 2007 / Published online: 18 July 2007

Abstract The biological rhythms of microalgal growth within a hydraulically integrated serial turbidostat algal reactor (HISTAR) were examined after comparison of a simple mechanistic productivity model with actual data yielded a standard error of prediction (SEP) of 62%. The data used for this study were taken on cultures of *Selenastrum capricornutum* grown under continuous 400-watt metal halide lighting. Fourier series analysis (up to five harmonics) was used to model the biorhythms and differentiate them from stochastic processes. Regression analyses revealed that the best Fourier series fit for the data was a three harmonic summation. Regression analyses on additional harmonic summations did not increase r^2 by more than 1%. The three harmonics were summed and incorporated into the growth term of the simple model, and the resultant full model was calibrated. The mechanistic HISTAR productivity model was greatly enhanced by the addition of the biological rhythm component, resulting in a SEP of <24.8 %. The period of the first harmonic was 13.4 days, which is very close to a circasemilunar rhythm (14.8 days). In summary, the predictive power of productivity models for continuous microalgal cultures can be dramatically improved with the inclusion of a biorhythm analysis.

B. C. Benson (✉)
Department of Renewable Resources,
University of Louisiana at Lafayette,
Lafayette, LA 70504, USA
e-mail: barbarabenson@louisiana.edu

M. T. Gutierrez-Wing · K. A. Rusch
Department of Civil and Environmental Engineering,
Louisiana State University,
Baton Rouge, LA 70803, USA

Keywords Circasemilunar rhythm · Harmonics · Mechanistic · Algae · Biomass

Abbreviations

μ_{max}	Maximum specific growth rate (day^{-1})
μ_n	Specific growth rate in reactor n (day^{-1})
μ_s	Hypothetical average system growth rate (day^{-1})
a_I	Coefficient of the cosine component of the k^{th} harmonic (k=1, 2, 3)
b_I	Coefficient of the sine component of the k^{th} harmonic (k=1, 2, 3)
CFSTR	continuous-flow, stirred-tank reactors
D_n	Local dilution rate for CFSTR n (day^{-1})
D_s	System dilution rate (day^{-1})
E_n	Elevation of the light source over $CFSTR_n$ (cm)
F_D	Factor representing the effect of D_s on growth rate
HISTAR	Hydraulically integrated serial turbidostat algal reactor
$I_{a\ n}$(PAR)	Average scalar irradiance in CFSTR n (μmol photons m^{-2} s^{-1})
I_{opt}(PAR)	Optimal scalar irradiance (μmol photons m^{-2} s^{-1})
k	Number of the harmonics
k_{en}	Decay rate in reactor n (day^{-1})
n	Numerical position of the specific CFSTR in the series
N	Total number of CFSTRs in HISTAR
η_t	Residual daily biomass concentration unaccounted for by harmonics (g dry wt m^{-3})
P	Periodic function that describes biorhythms
P_a	Areal productivity of HISTAR (g m^{-2} day^{-1})
P_{adj}	Proportional influence of the biorhythms on microalgal growth

R_I	Residual biomass concentration at time t (g dry wt m^{-3})
$\overline{R}$	Mid-point of the oscillations or mean of the residuals
t	Time (days)
t_{adj}	Adjustment required to synchronize minimum *p* value with spring tide
T	Total time (days)
T_p	Period (days)
V_n	Volume of $CFSTR_n$ (m^3)
W(t)	Mass loading per time period
X_{8a}	Actual biomass concentration in $CFSTR_8$ (g dry wt m^{-3})
X_{8p}	Predicted biomass concentration in $CFSTR_8$ (g dry wt m^{-3})
X_n	Concentration of biomass in CFSTR n (g dry wt m^{-3})
Y_o	Mid-point of the oscillations or mean

Introduction

Most prokaryotes and eukaryotes have an endogenous timekeeper (biological clock) that creates temporal order by governing the expressions of behavioral, physical, and biochemical rhythms (Roenneberg and Deng 1997; Staiger 1999). A geophysical timekeeper commonly referred to as a "zeitgeber" entrains most biological rhythms. The most common of these zeitgebers include the earth's rotation (24 h) and revolution around the sun (365 days), the moon's revolution around the earth (29 days), the rotation of the moon (24.8 h) and its effects on tidal fluctuation (12.4 h), and the combined effect of the sun's and moon's pulls, which cause the spring and neap tides (14.8 days). The rhythms entrained by these zeitgebers are referred to as circadian, circannual, circalunar, circatidal, and circasemilunar respectively (Rhee et al. 1981). The circadian is by far the most widely studied of the rhythms (Hasegawa et al. 1997; Allada et al. 1998; Gekakis and Wietz 1998). In contrast, the circasemilunar rhythm is the least studied of these rhythms, but is not without intrigue (Zeng et al. 1999).

Endogenous biorhythms help organisms, such as microalgae, with temporal orientation to their ecological setting (Hardeland 1997). Most organisms have evolved a variety of biorhythmic processes entrained on multiple zeitgebers, which help organisms temporally orient to changes in irradiance quality and quantity, nutrients, temperature, hydration, and seasonal meteorology (Roenneberg and Deng 1997). In algae, they have been reported to be responsible for cyclic changes in primary production (Lizon et al. 1998); phototaxis and vertical migration (Roenneberg and Deng 1997); fatty acid content (Molina Grima et al. 1994; Zhu et al. 1997; Acien Fernandez et al. 2000); carbon exchange, fixation, and storage (Kawamitsu and Boyer 1999); carbohydrates (Rebolloso Fuentes et al. 1999); and various metabolites such as melatonin (Hardeland 1997). Circadian rhythms orient algae to natural diurnal changes in temperature and irradiance (Roenneberg and Deng 1997), while circasemilunar rhythms orient microalgae to changes in mixing rates, salinity, nutrients, hydration, and irradiance caused by natural tidal fluxes (Kawamitsu and Boyer 1999; Lizon et al. 1998).

Circasemilunar rhythms follow the patterns of the neap and spring tides. Neap tides have the narrowest range and occur when the moon is at a right angle to the alignment of the earth and the sun. Spring tides have the greatest range (the highest high tides and lowest low tides) and they occur when the sun, earth, and the moon are in alignment (Moser and Macintosh 2001). The spring tides occur twice in a lunar month and cause occurrences of nutrient flushing and increased mixing rates in the upper estuary, hydration of the upper tidal zone (Lizon et al. 1998), and exposure and availability of light in the lower tidal zone (Kawamitsu and Boyer 1999). Various species have evolved reproductive and survival strategies to take advantage of these extreme tidal occurrences (Lizon et al. 1998; Oishi and Saigusa 1999; Wong and Townsend 1999; Zeng et al. 1999; Apollonio et al. 2002). Freshwater microalgal species, which evolved in the upper estuaries and fringing water bodies, are likely to be responsive to circasemilunar rhythms given the dynamic nature of this ecological origin.

While biological rhythms in natural systems, and in response to variation in irradiance, are recognized and well documented in the literature (Molina Grima et al. 1999; Camacho Rubio et al. 2003), little information on the role and impact of biological rhythms with zeitgebers other than irradiance is available for artificial microalgal production systems. As continuous microalgal cultures with long run times become increasingly more common for a variety of applications, system modeling will require a better understanding of biological rhythms to properly distinguish "true" stochastic system variability from cell synchronization trends. Circadian rhythms have been reported for several species of microalgae, e.g., *Gonyaulax polyedra* (Stein), *Emiliania hyxleyi* (Lohm), *Chlorella fusca* (Shihira and Krauss), *Chlorella sorokiniana* (Shihira and Krauss), and *Chlorella vulgaris* (Kessler and Huss) (Tischner and Lorenzen 1979; Poeggelet et al. 1991; Hardeland 1997; Roennberg and Deng 1997; Fritz 1999). The circadian synchronization of continuous microalgal cultures has become common practice for studying various aspects of cell developmental physiology (Tischner and Lorenzen

1979; Rhee et al. 1981; Thies and Grimme 1995; Fritz 1999). Physiological oscillations in *Gonyaulax* continue for several weeks in continuous conditions and can be entrained by several zeitgebers such as light and nutrients. Circannual rhythms have also been studied in plants such as sea grasses and several trees (Ramage and Schiel 1998; Callado et al. 2001). Previous efforts have mostly focused on these two types of rhythms. Individual biological rhythms can easily be modeled by a sinusoidal function. However, natural and biological systems may have multiple biological rhythms and other harmonics influencing the system such as seasonal inflows, predation and competition between species, and solar radiation. A Fourier series analysis can be used to identify and report various harmonics within systems and/or simulate periodic inputs with characteristics different from the typical sinusoidal function, i.e., half-sinusoid or pulse trains and seasonal or periodic loading (Chapra 1997; Sen et al. 2000).

The hydraulically integrated serial turbidostat algal reactor (HISTAR) was developed to provide for the continuous cultivation of microalgae (Rusch and Malone 1998; Rusch and Christenson 2003; Benson and Rusch 2006). A mechanistic model was developed to investigate and optimize the light dynamics with regard to system productivity within the culture reactors (Benson et al. 2007). The basic mass balance approach alone was not sufficient to describe the fluctuations in the biomass over time. Biomass in HISTAR does not reach a static steady state, but levels off to a steady-state phase characterized by defined fluctuations. The fluctuations of biomass in HISTAR, while appearing somewhat erratic in nature, tend to have some regularity of oscillation; suggesting that biological rhythms may play a part in the stochastic appearance of biomass production. The purpose of this research was to differentiate the significant biological rhythms, especially circasemilunar rhythms, from the stochastic fluctuations of microalgal growth within the HISTAR system and mathematically represent the effects of these rhythms on the specific growth rates within the overall mechanistic model.

Materials and methods

Experimental set-up

The HISTAR system consists of two automated sealed turbidostats (Rusch 1992; Rusch and Malone 1993; Rusch and Christensen 2003) hydraulically linked to a series of eight open, continuous-flow, stirred-tank reactors (CFSTRs) used to amplify the culture biomass (Fig. 1). Serial movement of the microalgae through the CFSTRs provides time for the culture to grow, reaching optimal density in the last CFSTR prior to harvest. The local retention time in each CFSTR (τ_n) is determined by the volume of the specific CFSTR (V_n) divided by the total flow (Q_T). The number of CFSTRs and τ_n determine the average cell residence time in the system (τ_s) (Rusch and Malone 1998). An in-depth discussion of the theory and system description can be found in Rusch and Malone (1998), Theegala et al. (1999), and Rusch and Christenson (2003).

Productivity data from a suite of experiments performed at four different system dilution rates $\left(D_s = t_s^{-1};\ 0.264,\ 0.385,\ 0.642,\ and\ 1.127^{-1}\right)$ were used to differentiate the significant biological rhythms from the stochastic fluctua-

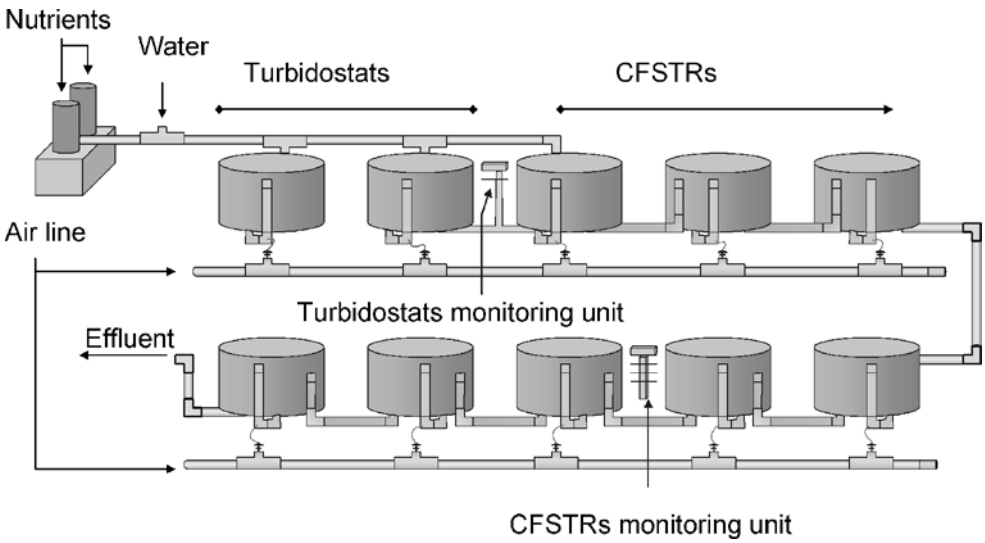

Fig. 1 The hydraulically integrated serial turbidostat algal reactor (HISTAR) system (3,570-l culture volume) consists of two sealed turbidostats and the eight continuous-flow, stirred-tank reactors (CFSTRs)

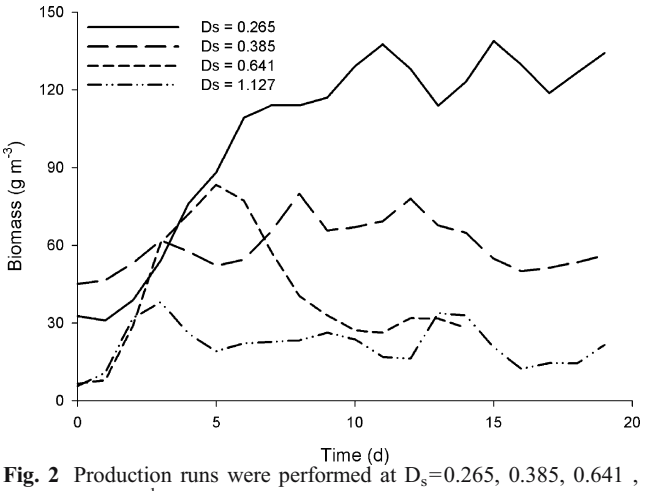

Fig. 2 Production runs were performed at D_s=0.265, 0.385, 0.641 , and 1.127 day^{-1}. Illustrated here are the biomass concentrations in $CFSTR_8$ over time for each of the runs

tions of microalgal growth within HISTAR (Fig. 2). The data were collected using *Selenastrum capricornutum* Printz (UTEX 1648), a ubiquitous eurytopic microalgae common to the freshwaters of the lowlands (Shubert 1984). The culture was grown under continuous lighting from 400-W metal halide lamps (one per reactor; Philips Lighting Company, model MH400/U) equipped with a collimating plate to focus the light beam as perpendicular to the culture surface as possible. The culture temperature was maintained at 27±1.5°C. CO_2 was injected as needed every 10 min to maintain the pH at 7.5±0.5. Adjustments to the dosing time were made using feedback from the pH probe to the process control system. Nutrients (F/2 Algal Culture Formula; Kent Marine, Franklin, WI, USA) were continuously fed into the in-flowing water line at a drip rate of 0.2 mL min^{-1} to maintain a target of approximately 4 mg NO_3-N L^{-1} and 2.25 mg PO_4-P L^{-1}. The air flow into the airlift tubes was maintained at 2.1 m^3 h^{-1}, resulting in a water recirculation flow rate of 36 L min^{-1} per reactor. The culture depth was 0.64 m for each reactor. Biomass densities within each reactor were automatically estimated every hour by a biomass sensor, which generated a millivolt signal in response to the amount of microalgae in the reactor. The millivolt signal was transmitted to the process control system and converted to g dry wt m^{-3} via a standard curve. Daily productivity was calculated by multiplying the biomass concentration in $CFSTR_8$ by D_s.

Productivity model

A mechanistic model was developed to facilitate investigation of various production scenarios of HISTAR system behavior. A complete description of this model can be found in Benson et al. (2007), while a short discussion of the growth rate parameter is presented in this paper as background for the biorhythm analysis. The governing equation for system productivity within the HISTAR system can be written as:

$$\frac{\partial X_n}{\partial t} V_n = Q_T X_{n-1} - Q_T X_n + \left[\left(\mu_{\max} [(1-P) P_{adj}] [F_D] \left[\frac{I_{an}(PAR)}{I_{opt}(PAR)} \cdot e^{\frac{-I_{an}(PAR)}{I_{opt}(PAR)}+1} \right] \right) - k_{e_n} \right] X_n V_n \quad (1)$$

The growth rate was initially modeled using Steele's equation and a parameter (F_D) that represents the effects of self-shading on the culture. Initial attempts at model calibration brought to light excessive model error. Daily biomass levels in HISTAR exhibited erratic variation over time even long after steady state was reached (Fig. 2). These fluctuations, at first glance, appeared to be due to the stochastic nature of HISTAR, which is expected of all biological systems. However, due to what appeared to be regularity in the complex oscillations of biomass concentration, biological rhythms were considered to be potential contributors to the variations in biomass. Circadian rhythms were not investigated during this study and were eliminated from consideration by using mean daily biomass data.

Fourier series analysis

Fourier series analysis was used to investigate the discrepancies between the productivity model simulations and experimental data. A Fourier series involves the summing of harmonics within a system:

$$W(t) = a_o + \sum_{i=1}^{\infty} \left[a_I \cos\left(i \frac{2\pi}{T_p} t \right) + b_i \sin\left(i \frac{2\pi}{T_p} t \right) \right] \quad (2)$$

Once solved, this equation can be substituted into a mass balance equation of a system to explain and simulate periodic inflows to that system due to loading or growth. Data examined for the possible existence of periodic components such as biorhythms or seasonal inflows must first be transformed to remove all other known effects or trends, with the residuals representing only the periodic deterministic components and the stochastic components (Sen et al. 2000). By adding a phase shift parameter ($\pi/2$) to the second term in Eq. 2, the cosine function can be expressed as a sine function. For modeling oscillations in

residual biomass concentration over time, the Fourier equation can be expressed as follows:

$$R_i = \overline{R} + \sum_{i=1}^{k}\left[a_i \sin\left(i\frac{2\pi}{T_p}t + \frac{\pi}{2}\right) + b_i \sin\left(i\frac{2\pi}{T_p}t\right)\right] + \eta_t (t = 1, 2, \ldots T) \quad (3)$$

The remaining residuals are the last term of Eq. 3 and represent the stochastic component of the system. Equation 3 can then be used to model the periodic nature and remaining stochastic nature of a biological system (Sen et al. 2000). If the last term is insignificant due to insignificant amplitude of the stochastic residuals remaining after the harmonics are removed from the data, the stochastic nature of errors can be ignored.

The first step to using the Fourier process involved transformation of the data to remove any responses of mechanistic or other deterministic (non-harmonic) trends. A simple mechanistic productivity model was developed to represent these other processes, i.e., mass balance, light effects on growth rate, and inflow from the turbidostats to the CFSTRs (Benson et al. 2007). This simple model had a near static (almost free of fluctuations) steady state, which did not represent the observed periodicity in the data. Once the simple model was complete (i.e., fully calibrated, but without a biological rhythm component—from here forward referred to as simple model), a simulation was run for a 19-day period (average duration of the experimental runs). The simple model simulation was compared with an actual set of daily mean biomass concentrations from one of the experimental runs in HISTAR (D_s=0.385 day^{-1}). Only biorhythms with periods longer than 1 day were observable since daily averaging removed any circadian rhythms from the data. A comparison between the simulation results of the simple productivity model and the actual daily biomass concentrations generated a set of residuals. The standard error of prediction (SEP) was determined and represented on a percent basis by dividing the SEP by the mean of the actual data (Draper and Smith 1981). The acceptable standard error of prediction was 25%. However, the calculated SEP for this comparison was 62% and deemed unacceptable.

A Fourier series analysis was performed on these residuals using a base period (T_p) of 14.79 days. Regression analyses were completed on the Fourier series with one to five harmonics. The longest harmonic summation to increase r^2 by more than 1% was used in the model. This harmonic summation was incorporated into the simple model as the periodicity term (P) effect on growth rate (from here forward referred to as full model). Analyses were performed in Tablecurve 2 D (v.5.01; Systat Software, San Jose, CA, USA, 2002).

Model calibration and validation

The full model was calibrated against biomass concentrations from $CFSTR_8$ collected at D_s=0.386, 0.265 ,and 1.127 day^{-1}. The model parameters determined to be the most sensitive were T_p and F_D. The base period was adjusted to obtain the lowest standard error for the three series, while F_D was calibrated for each data set. Attempts were made to validate the productivity model by comparison with another data set collected at Ds=0.642 day^{-1}. Standard error of predictions were calculated for the three calibration data sets, the final calibrated model, and the validation attempt.

Results and discussion

A comparison of the simulation results from the simple model and the actual $CFSTR_8$ daily biomass concentrations at D_s=0.385 day^{-1} resulted in residuals ranging from 8.36 to 43.11 g dry wt m^{-3} (Fig. 3). These residuals illustrated a sinusoidal shape with a period approaching 14.8 days, which corresponds with a circasemilunar rhythm (Fig. 4). Regression analyses on the successive summation of the harmonics indicated that harmonics 4 and 5 did not increase r^2 by more than 1%. Thus, further analyses were limited to harmonics 1–3. The Fourier series analysis of these initial residuals resulted in sinusoidal functions representing the first harmonic (Fig. 4), the first and second harmonics

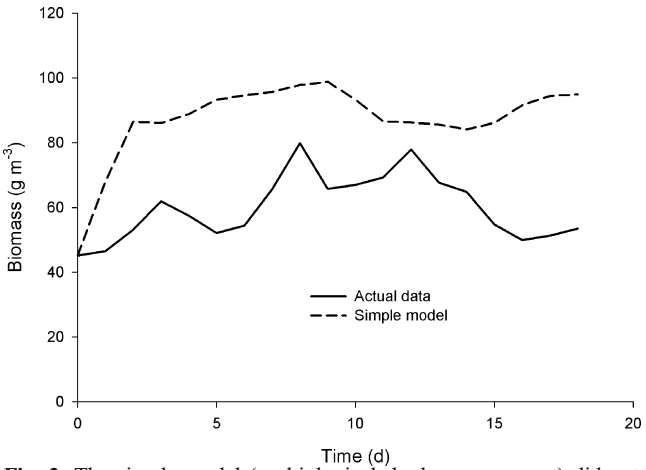

Fig. 3 The simple model (no biological rhythm component) did not compare well with the actual $CFSTR_8$ biomass data for D_s= 0.385 day^{-1}

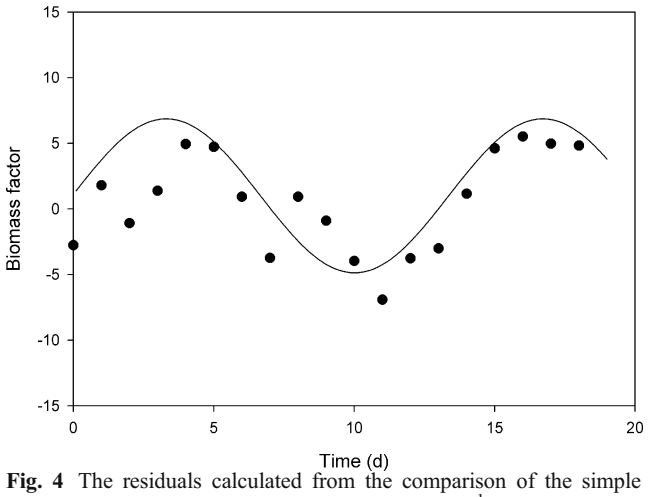

Fig. 4 The residuals calculated from the comparison of the simple model and the experimental data for D_s=0.385 day^{-1} were plotted and regressed against the first harmonic of the Fourier series analysis

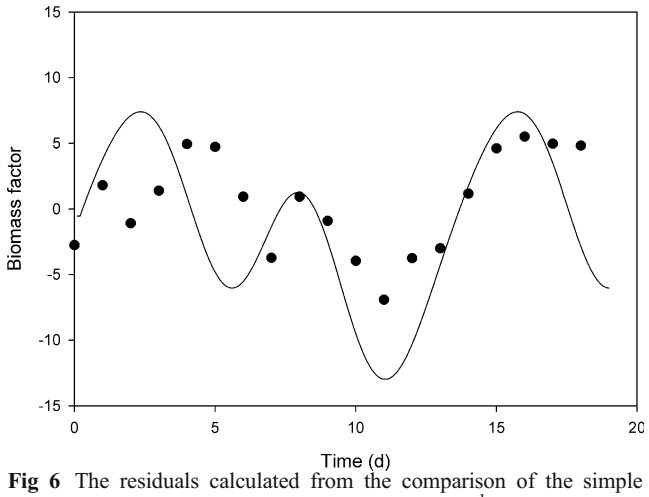

Fig 6 The residuals calculated from the comparison of the simple model and the experimental data for D_s=0.385 day^{-1} were plotted and regressed against the summation of the first, second, and third harmonics of the Fourier series analysis

summed (Fig. 5), and all three harmonics summed (Fig. 6). The best Fourier series fit for the data was determined to be the three-harmonic summation with a T_p=14.79 days.

The three harmonics were summed and incorporated into the simple model as parameter P:

$$P = y_O + \sum_{I=1}^{3} \left[a_i \sin\left(i2\pi \frac{t+t_{adj}}{T_p} + \frac{\pi}{2} \right) \right] + \left[b_i \sin\left(i2\pi \frac{t+t_{adj}}{T_p} \right) \right] \quad (4)$$

resulting in the full model, which was fully calibrated. Prior to calibration, time (t) was adjusted (t_{adj}) to match the spring tides at the time the data were collected (Weeks Bay and Vermilion Bay, LA, USA; http://www.harbortides.com/tidetable.asp) [2001]. Equation 4 was developed from oscillations in X_n, not μ_n. It was assumed that the fluctuations in biomass modeled by P were caused by, and therefore, proportional to, biorhythms in μ_n. Therefore, P was multiplied by a proportional adjustment factor (P_{adj}) to represent the effects the biorhythms have on μ_n. P_{adj} is a ratio of the dilution flow (Q_f) and the total flow (Q_T). In the productivity model, parameter P was a term in the individual specific growth rate term (μ_n) of each CFSTR mass balance. The resulting specific growth rate term (see Eq. 1) comprises three components: harmonics representing biorhythms (P), effects of self-shading (F_D), and effects of average scalar irradiance (I_{an}(PAR)). The estimated values of the full model parameters and the final calibrated values are summarized in Table 1. The most interesting of these values is that of the period length, T_p, which was estimated to be 14.79 days and was calibrated to 13.4 days. This is still close to the anticipated circasemilunar period of 14.8 days observed in nature, which represents the rhythm of the spring and neap tides and is sometimes reported in organisms of the upper tidal zone. The three individual harmonics and their summation were represented as graphs for observational purposes (Fig. 7).

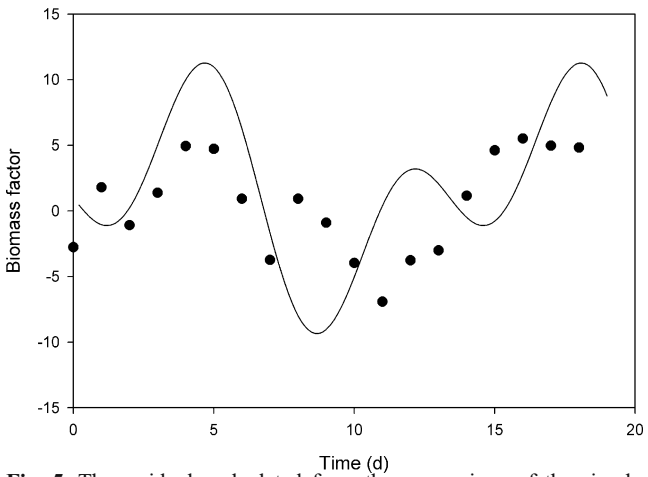

Fig. 5 The residuals calculated from the comparison of the simple model and the experimental data for D_s=0.385 day^{-1} were plotted and regressed against the summation of the first and second harmonics of the Fourier series analysis

Results from simple and final model simulations for D_s= 0.385 day^{-1} and the actual data were plotted together to provide an illustrative example of the positive impact of including biorhythms when modeling biological systems (Fig. 8). The addition of P to the productivity model resulted in a better fit (mean SEP=18.23%, range =16.5–19.4%) of the experimental data for D_s=0.265, 0.385, and 1.127 day^{-1}. Recall that the SEP was 62% for the simple model. With the addition of the biological rhythm component, the final model represents the actual data fairly well (Fig. 8). The oscillations of the final model are complicated by inconsistent inputs and fluctuating mass transfer from the turbidostats into $CFSTR_1$. These stochastic inputs erratically fluctuate, causing the model to do so. This gives

Table 1 The estimated parameters of the productivity model for hydraulically integrated serial turbidostat algal reactor (HISTAR)

Parameter	Theoretically calculated or experimental estimation	Final calibrated parameters	Literature values
Light parameters			
I_{Eon} (PAR) (μmol photons m^{-2} s^{-1})	597.7	Not adjusted	Unique to HISTAR
k_a (μmol photons m^{-2} s^{-1}) cm^{-1}	7.464	Not adjusted	Unique to HISTAR
k_w (m^{-1})	1.97	Not adjusted	0.001 (Molina Grima et al. 1994) for $k_0 = k_w + k_b X$
k_b ($m^2 g^{-1}$)	0.0575		
Growth parameters			
μ_{max} (day^{-1})	1.73	Not adjusted	1.85 (Toerien and Huang 1973)
I_{opt} (PAR) (μmol s^{-1} m^{-2})	355.5	Not adjusted	345–1,125 (Lester et al. 1988)
F_D (dimensionless)			Unique to HISTAR
If : D_s=0.265	0.540	0.533	
D_s=0.385	0.594	0.428	
D_s=0.641	1.187	0.830	
D_s=1.127	0.952	0.937	
k_{en} (day^{-1})			0.1 (Jorgensen 1988)
If : D_s=0.265	0.278	Unique to each dilution and CFSTR	
D_s=0.385	0.100		
D_s=0.641	0.042		
D_s=1.127	0.020		
Periodicity parameters (P)			Unique to HISTAR
Y_0	0.555	Not adjusted	
T_p	14.79	13.40	
First harmonic (pr_1)			
a_1	0.237	Not adjusted	
b_1	4.720	Not adjusted	
Second harmonic (pr_2)			
a_2	2.837	Not adjusted	
b_2	0.325	Not adjusted	
Third harmonic (pr_2)			
a_3	−0.189	Not adjusted	
b_3	−0.611	Not adjusted	
Combined harmonics			
T_{adj}	Unique to each data set; adjusts model to local spring tide		
P_{adj}	(Q_f/Q_f+Q_{tb}) /8		

CFSTR: continuous-flow, stirred-tank reactor

the simulation of the final productivity model an erratic appearance. However, the error remaining is low enough to eliminate the need for including a stochastic component in the growth rate term of the model. The validation process using the D_s=0.641 day^{-1} data set resulted in a SEP= of 46.6%. While an SEP of 46% is not unusual for biological systems, it did not meet the 25% standard set by the authors. Subsequently, this data set was included in the calibration process, resulting in an overall mean SEP of 25% for the four data sets.

At first glance, the model would appear erratic in nature without understanding the complex internal rhythms it represents. The period length is close to that of the circasemilunar biological rhythm. In nature, the extreme spring tide would be a time when nutrients would be flushed into the upper estuaries and fringing freshwater areas and the dilution and mixing rates of these areas would be increased. Such areas may only be affected by the extreme nature of spring tides and not by the subtle daily tides. Synchronization of maximum endogenous growth

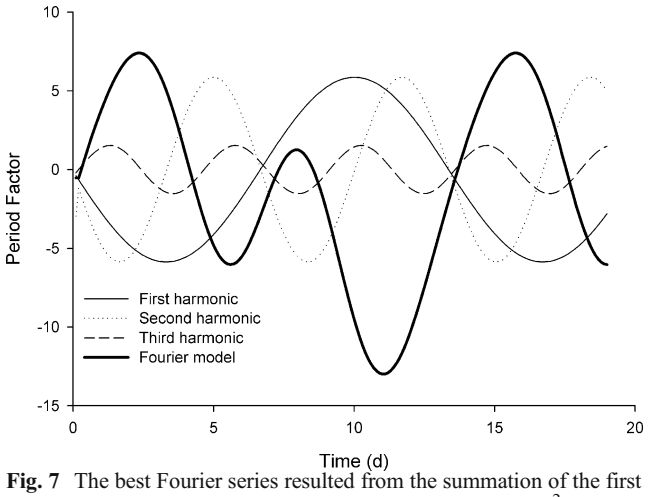

Fig. 7 The best Fourier series resulted from the summation of the first three harmonics. Additional harmonics did not increase the r^2 by more than 1%

potential with a time that nutrients, irradiance, mixing, and habitat are plentiful would be a good evolutionary strategy for a microalgal species in this type of ecosystem. Therefore, the existence of circasemilunar rhythms in the microalgal productivity data is understandable.

Although asynchronous cultures are usually preferred in commercial production settings because of their steady productivity, synchronous cultures may produce certain biochemical products at certain points in their cycle. Modeling and understanding culture periodicity may facilitate management of undesirable biomass fluctuations in synchronized cultures and help determine the cropping time for biomass when specific products have been maximized.

In conclusion, the Fourier series analysis was useful in identifying and modeling circasemilunar biological rhythms within a microalgal culture in HISTAR. The final mechanistic model was greatly enhanced by the addition of the biological rhythm component. This new understanding of the biological rhythms of *S. capricornutum* growth in HISTAR will greatly enhance the predictability of microalgal productivity from the system. Caution should be used when applying this model to other species because different species respond differently to different zeitgebers. It will be necessary to determine the biological rhythms of the organisms of concern and incorporate them into the model using the Fourier methodology described in this paper. However, considering biorhythms in the modeling of microalgal productivity can significantly enhance the accuracy of productivity forecasting. Asynchronous cultures are usually preferred for stable productivity in commercial realms; however, maintaining sustained asynchronous conditions is difficult. Therefore, understanding the periodicity of microalgal productivity can facilitate better management of synchronized cultures.

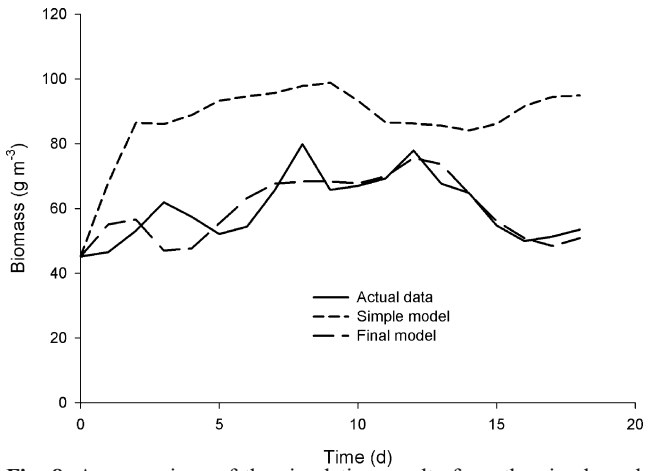

Fig. 8 A comparison of the simulation results from the simple and final models clearly shows the positive impact of the harmonic analysis (data for D_s=0.385 day^{-1})

References

Acien Fernandez FG, Sanchez Perez JA, Fernandez Sevilla JM, Garcia Camacho F, Molina Grima E (2000) Modeling of eicosapentaenoic acid (EPA) production from *Phaeodactylum tricornutum* cultures in tubular photobioreactors: effects of dilution rate, tube diameter, and solar irradiance. Biotechnol Bioeng 68:173–183

Allada R, Hall J, Rosbash M (1998) A mutant *Drosophila* homolog of mammalian clock disrupts circadian rhythm and transcription of period and timeless. Cell 93:791–804

Apollonio S, Pennington M, Cota G (2002) Simulation of phytoplankton photosynthesis by bottom-ice extracts in Arctic. Springer, Heidelberg, pp 1–5

Benson B, Rusch K (2006) Investigation of the light dynamics and their impact on algal growth rate in a hydraulically integrated serial turbidostat algal reactor (HISTAR). J Aquac Eng 35:122–134

Benson B, Gutierrez-Wing M, Rusch K (2007) The development of a mechanistic model to investigate the impacts of the light dynamics on algal productivity in a hydraulically integrated serial turbidostat algal reactor (HISTAR). J Aquac Eng 36:198-211

Callado C, da Silva Neto S, Scarano F, Costa C (2001) Periodicity of growth rings in some flood-prone trees of the Atlantic rain forest in Rio de Janeiro, Brazil. Trees 15:492–497

Camacho Rubio F, Garcia Camacho F, Fernandez Sanchez JM, Chisti Y, Molina Grima E (2003) A mechanistic model of photosynthesis in microalgae. Biotechnol Bioeng 81:459–473

Chapra S (1997) Surface water-quality modeling. McGraw-Hill, New York

Draper NR, Smith H (1981) Applied regression analysis. Wiley, New York

Fritz J (1999) Carbon fixation and coccolith detachment in the coccolithophore *Emiliania huxleyi* in nitrate-limited cyclostats. Mar Biol 133:509–518

Gekakis N, Wietz C (1998) Role of the CLOCK protein in the mammalian circadian mechanism. Science 280:1564–1576

Harbortides (2001) http://www.harbortides.com/tidetable.asp?Station=2303&period=-7. Accessed 25 December 2001

Hardeland R (1997) New actions of melatonin and their relevance to biometeorology. Int J Biometeorol 41:47–57

Hasegawa K, Tsukahara Y, Shimamoto M, Matsumoto K, Nakaoka Y, Sato T (1997) The Paramecium circadian clock: synchrony of

changes in motility, membrane potential, cyclic AMP and cyclic GMP. J Comp Physiol A 181:41–46
Jorgensen S (1988) Fundamentals of ecological modeling. Elsevier, Amsterdam, pp 1–391
Kawamitsu Y, Boyer J (1999) Photosynthesis and carbon storage between tides in a brown alga, *Fucus vesiculosus*. Mar Biol 133: 361–369
Lester WW, Adams MS, Farmer AM (1988) Effects of light and temperature onphotosynthesis of the nuisance alga*Cladophora glomerata* (L.) Kutz from GreenBay, Lake Michigan. New Phytol 109:53–58
Lizon F, Seuront L, Lagadeuc Y (1998) Photoadaptation and primary production study in tidally mixed coastal waters using a Lagrangian model. Mar Ecol Prog Ser 169:43–54
Molina Grima E, Sanchez Perez JA, Garcia Camacho F, Garcia Sanchez JL, Acien Fernandez FG, Lopez Alonso D (1994) Outdoor culture of *Isochrysis galbana* ALII-4 in a closed tubular photobioreactor. J Biotechnol 37:158–166
Molina Grima E, Acien Fernandez FG, Garcia Camacho F, Chisti Y (1999) Photobioreactors: light regime, mass transfer, and scaleup. J Biotechnol 70:231–247
Moser S, Macintosh D (2001) Diurnal and lunar patterns of larval recruitment of Brachyura into a mangrove estuary system in Ranong Province, Thailand. Mar Biol 138:827–841
Oishi K, Saigusa M (1999) Rhythmic patterns of abundance in small sublittoral crustaceans: variety in the synchrony with day/night and tidal cycles. Mar Biol 133:237–247
Poeggelet B, Blazer, Hardeland R, Lerchl A (1991) Pineal hormone melatonin oscillates also in the dinoflagellate *Gonyaulax polyedra*. Naturwissenschaften 78:268–269
Ramage D, Schiel D (1998) Reproduction in the seagrass *Zostera novazelandica* on intertidal platforms in southern New Zealand. Mar Biol 130:479–489
Rebolloso Fuentes MM, Garcia Sanchez JL, Fernandez Sevilla JM, Acien Fernandez FG, Sanchez Perez JA, Molina Grima E (1999) Outdoor continuous culture of *Porphyridium cruentum* in a tubular photobioreactor: quantitative analysis of the daily cyclic variation of culture parameters. J Biotechnol 70:271–288
Rhee G, Gotham I, Chisholm S (1981) Use of cyclostat cultures to study phytoplankton ecology. In: Calcott PH (ed) Continuous culture of cells. CRC, Boca Raton
Roenneberg T, Deng T (1997) Photobiology of the *Gonyaulax* circadian system: Different phase response curves for red and blue light. Planta 202:494–501
Rusch KA (1992) Demonstration of a control strategy for sustained algal growth at a full-scale level under computer automated, continuous culture conditions. Dissertation, Louisiana State University
Rusch K, Christenson J (2003) The hydraulically integrated serial turbidostat algal reactor (HISTAR) for microalgal production. J Aquac Eng 27:249–264
Rusch K, Malone R (1993) Bench-scale evaluation of a micro-computer automated algal turbidostat. J World Aquac Soc 24:379–389
Rusch K, Malone R (1998) Microalgal production using a hydraulically integrated serial turbidostat algal reactor (HISTAR): a conceptual model. J Aqua Eng 18:251–264
Sen Z, Kadilglu M, Batur E (2000) Stochastic modeling of the Van Lake monthly level fluctuations in Turkey. Theor Appl Climatol 65:99–110
Shubert L (1984) Algae as ecological indicators. Academic, London
Staiger D (1999) The circadian system of *Arabidopsis thaliana*: forward and reverse genetic approaches. Chronobiol Int 16:1–16
Systat Software (2002) Tablecurve 2D v.5.01 Software
Theegala C, Malone R, Rusch K (1999) Contaminant washout in a hydraulically integrated serial turbidostat algal reactor (HISTAR). J Aquac Eng 19:223–241
Thies F, Grimme L (1995) O-Dealkylation of coumarin and resorufin ethers by unicellular green algae: kinetic properties of *Chlorella fusca* and *Chlorella sorokiniana*. Arch Microbiol 164:203–211
Tischner R, Lorenzen H (1979) Nitrate uptake and nitrate reduction in synchronous *Chlorella*. Planta 146:287–292
Toerien DF, Huang CH (1973) Algal growth prediction using growth kinetic constants.Water Res 7:1673–1681
Wong M, Townsend D (1999) Phytoplankton and hydrography of the Kennebec estuary, Maine, USA. Mar Ecol Prog Ser 178:133–144
Zeng C, Abello P, Naylor E (1999) Endogenous tidal and semilunar molting rhythms in early juvenile shore crabs *Carcinus maenas*: implications for adaptation to a high intertidal habitat [abstract]. Mar Ecol Prog Ser 191:257–266
Zhu C, Lee Y, Chao T, Lim S (1997) Diurnal changes in gross chemical composition and fatty acid profiles of *Isochrysis galbana* TK1 in outdoor closed tubular photobioreactors. J Mar Biotechnol 5:153–157